Sensor and Simulation Notes

Note 449

August 2000

Design and Numerical Simulation of the Response of a Coaxial Beam-Rotating Antenna Lens

Clifton C. Courtney, Donald E. Voss and Michael Thomas
Voss Scientific
Albuquerque, NM

Carl E. Baum, William Prather, and Robert Torres
Air Force Research Laboratory / Directed Energy Directorate
Kirtland Air Force Base, NM

ABSTRACT

Previous embodiments of the Coaxial Beam-Rotating Antenna (COBRA) have utilized offset surfaces to realize ray path length differences. These path length differences transform an azimuthally symmetric aperture field distribution to a form that produces a centrally peaked radiation pattern with linear or circular polarization. The same aperture transformation can be achieved with a lens that covers the aperture of a conical horn antenna driven in the TM_{01} circular waveguide mode. The analysis, design, and numerical simulation of COBRA lenses are summarized in this note. The first section will review the design principles associated with a collimating lens design, then introduce the COBRA lens concept. The discussion of the lens design also includes a technique for reducing multiple reflections in the lens which otherwise would reduce the desirable radiating characteristics. Next, an example of a lens design is presented. Finally, the results of finite-difference time domain (FDTD) numerical simulations of the response of COBRA lens designs are presented. It is shown that the radiated pattern of a conical horn antenna, driven by the TM_{01} circular waveguide mode, can be made to exhibit a boresight null (no lens), a boresight peak with linear polarization (N = 2 COBRA lens), or a boresight peak with circular polarization (N = 3 or 4 COBRA lens) when outfitted with an appropriate COBRA Lens.

Acknowledgement - This work was supported in part by the Air Force Office of Scientific Research, and in part by the Air Force Research Laboratory, Directed Energy Directorate, under a Small Business Innovation for Research (SBIR) Phase II program, Contract No. F29601-97-C-0005.

Table of Contents

Table of Figures

1. INTRODUCTION

Previous embodiments of the Coaxial Beam-Rotating Antenna (COBRA) have utilized offset surfaces to realize ray path length differences. These path length differences transform an azimuthally symmetric aperture field distribution to a form that produces a centrally peaked radiation pattern with linear or circular polarization. Examples of these types of antennas are discussed in the literature [Ref. 1 - 6].

The same aperture transformation can be achieved with a lens that covers the aperture of a conical horn antenna driven in the TM_{01} circular waveguide mode. Whereas the stepped reflecting surfaces altered the physical path length (and correspondingly the electrical path length), the Lensed COBRA alters the electrical path length with the judicious use of dielectric material.

The analysis, design, and simulation of a COBRA lens are presented in this note. The first section presents the analysis and fundamental design equations. It also includes a review of a collimating lens design. The presentation also includes a technique for reducing multiple reflections in the lens which otherwise would reduce the desirable radiating characteristics. In the next section examples of lens design are presented. Finally, the results of finite-difference time domain (FDTD) simulations of several COBRA lens designs are presented. It is shown with FDTD simulations that the radiated pattern of a conical horn antenna, driven by the TM_{01} circular waveguide mode, can be made to exhibit a boresight null (no lens), a boresight peak with linear polarization (N = 2 COBRA lens), or a boresight peak with circular polarization (N = 3 or 4 COBRA lens).

2. LENS DESIGN

2.1 General Design of a Microwave Lens

In Figure 1 there is shown the geometry of a standard collimating microwave lens [Ref. 7]. The lens is composed of a material with relative dielectric constant ε. A point source is shown located at the position indicated by o which is a distance f from the rear surface of the lens. The challenge is to derive an expression for the surface that yields an equivalent optical path length through the lens. If this is so, then the front surface of the lens will be an equi-phase surface. With this in mind we can write the relation

$$f + \sqrt{\varepsilon}\, t = r + \sqrt{\varepsilon}\, \overline{BC} \tag{2.1}$$

where $\overline{BC}$ = physical path length between points B and C. Since $t = r\cos\theta - f + \overline{AD}$, and $\overline{AD} = \overline{BC}$ the above can be written as

$$f + \sqrt{\varepsilon}\,(r\cos\theta - f) = r$$

or,

$$r = \frac{(\sqrt{\varepsilon} - 1) f}{\sqrt{\varepsilon} \cos\theta - 1}, \tag{2.2}$$

which is the equation of a hyperboloidal surface. Note that the maximum value of the angle is $\theta_{max} = \cos^{-1}(1/\sqrt{\varepsilon})$ which then defines the lens radius as

$$2a = \frac{2(\sqrt{\varepsilon} - 1) f \cos\theta_{max}}{\sqrt{\varepsilon} \sin\theta_{max} - 1} \tag{2.3}$$

The lens F-number is defined as

$$F = f / 2a \tag{2.4}$$

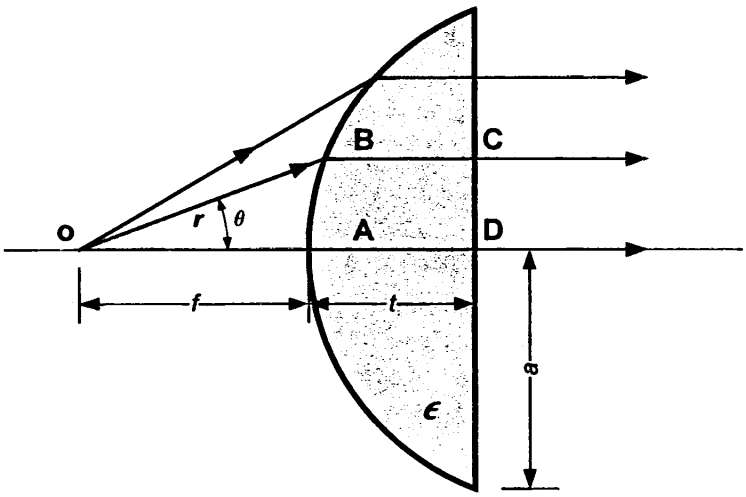

Figure 1. The geometry of a microwave lens.

2.2 *Use of a Microwave Lens with a Conical Horn Antenna*

The microwave lens described in the last section can be used to collimate the aperture field of a conical horn antenna. In Figure 2 is shown a circular waveguide (diameter = $2r$) that is terminated in a conical horn antenna (length = l, aperture diameter = $2a$). The phase center of the antenna is assumed (approximated) to be located on the axis of the guide at the interface between guide and the horn. A lens with a material of relative dielectric constant ε_r fits in the aperture at the end of the conical horn. The lens parameters are as follows. The required lens focal length is

$$f = \frac{2r(\sqrt{\varepsilon_r} \cos\theta - 1)}{\sqrt{\varepsilon_r} - 1)}. \tag{2.6}$$

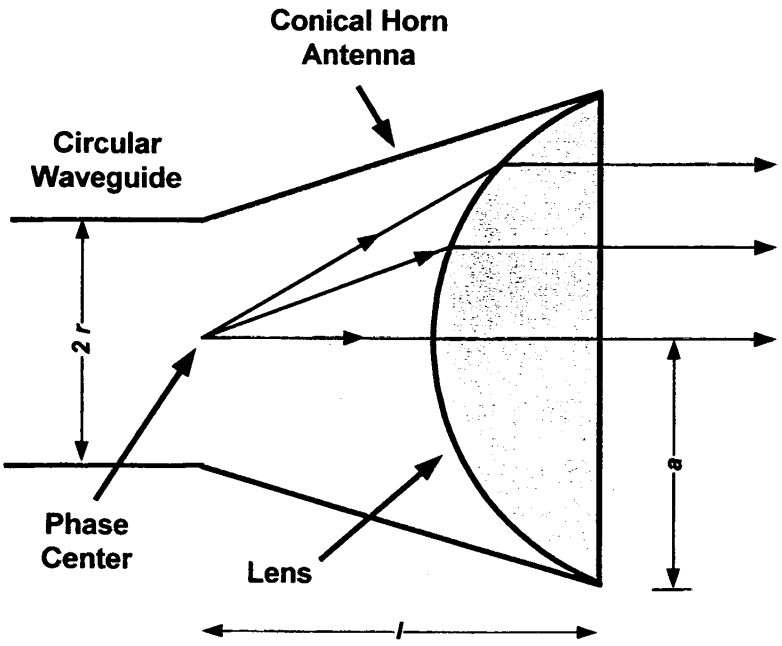

Figure 2. A microwave lens is fitted in the aperture of a conical horn antenna.

2.3 COBRA Lens Analysis and Design

The general design of a COBRA lens is dictated by the need to advance or retard the phase of the aperture field by a prescribed amount. To do so the lens geometry is defined simply by the requirement that the optical path length is altered, by adding additional dielectric material, in a prescribed manner. Specifically, the phase difference between lens sectors is given by

$$\Delta\varphi = \frac{2\pi(n-1)}{N} \qquad \text{for } n = 1,2,\ldots,N. \tag{2.7}$$

where N = number of steps in the lens surface. For this phase difference to be accomplished the sector step size must be given by the following

$$\Delta\varphi = \frac{2\pi(n-1)}{N} = \beta l\sqrt{\varepsilon_r} - \beta l = \beta l(\sqrt{\varepsilon_r} - 1). \tag{2.8}$$

The step size is then

$$\Delta l = \frac{1}{N}\frac{\lambda}{\sqrt{\varepsilon_r} - 1}, \tag{2.9}$$

and the thickness of each sector is

$$l_n = \frac{2\pi(n-1)}{N}\frac{1}{\beta\left(\sqrt{\varepsilon_r}-1\right)} = \frac{(n-1)}{N}\frac{\lambda}{\sqrt{\varepsilon_r}-1}, \quad \text{for } n = 1,2,\ldots,N. \qquad (2.10)$$

The general geometry of an N = 4 COBRA lens is shown in Figure 3. Two examples are next given to demonstrate use of the design equation.

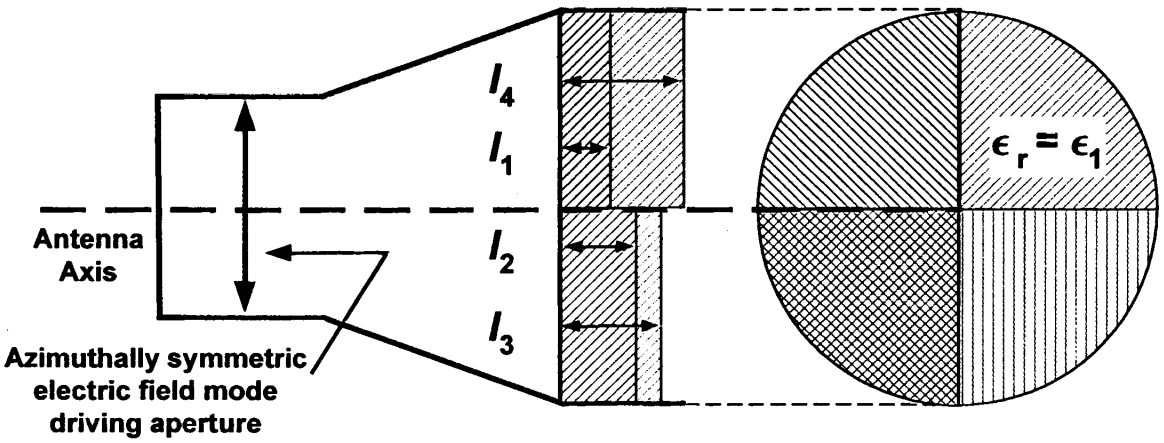

Figure 3. The geometry of an N = 4 COBRA lens.

Let $N = 2$, and the operating frequency = 1.3 GHz. For a lens dielectric constant of $\varepsilon_r = 2.5$ the lens step size will be

$$\Delta l = \frac{1}{2}\frac{\lambda}{\sqrt{\varepsilon_r}-1} = 0.86\lambda \qquad (2.11)$$

The thickness of each sector will be

$$l_1 = 0, \qquad (2.12a)$$

and

$$l_2 = \frac{\lambda}{2}\frac{1}{\sqrt{\varepsilon_r}-1} = 0.86\lambda. \qquad (2.12b)$$

This lens will produce a bore sight peak with linear polarization.

Next, let $N = 4$, and the operating frequency is 1.3 GHz. The lens dielectric constant is specified as $\varepsilon_r = 2.5$. The lens step size will be

$$\Delta l = \frac{1}{4}\frac{\lambda}{\sqrt{\varepsilon_r}-1} = 0.43\lambda \tag{2.13}$$

The thickness of each sector will be

$$l_1 = 0, \tag{2.14a}$$

$$l_2 = \frac{2\pi}{4}\frac{\lambda}{2\pi\left(\sqrt{\varepsilon_r}-1\right)} = \frac{\lambda}{4}\frac{1}{\sqrt{\varepsilon_r}-1} = 0.43\lambda, \tag{2.14b}$$

$$l_3 = \frac{2\pi(2)}{4}\frac{\lambda}{2\pi\left(\sqrt{\varepsilon_r}-1\right)} = \frac{\lambda}{2}\frac{1}{\sqrt{\varepsilon_r}-1} = 0.86\lambda, \tag{2.14c}$$

and

$$l_4 = \frac{2\pi(3)}{4}\frac{\lambda}{2\pi\left(\sqrt{\varepsilon_r}-1\right)} = \frac{3\lambda}{4}\frac{1}{\sqrt{\varepsilon_r}-1} = 1.29\lambda. \tag{2.14d}$$

This lens will also produce a bore sight peak with circular polarization.

2.4 *Impedance Matching of the COBRA Lens*

The use and shape of the dielectric material serves to focus (or collimate) the propagating electromagnetic field and mode convert the aperture field. It also causes wave reflections at the front and back lens interfaces due to an impedance mismatch caused by the difference in the dielectric constant between the regions with and without the lens. Reflections occur at both the interior and exterior interfaces. But it is the exterior interface which is most problematic. Reflections that occur at the interior interface cause reflected microwave energy to be directed back toward the source, and if the source is matched to the guide this microwave energy does not come back to the aperture area (it is dissipated in the source impedance). However, reflections that occur at the exterior surface "rattle" around in the lens and cause perturbations in the magnitude and phase of the aperture distribution over the lens. Consequently, it is desired to "impedance match" the exterior interface to eliminate these reflections on the exterior side of the lens.

Fortunately the procedure to impedance match the exterior interface is straight forward. Let Z_0 = free space impedance, and let Z_1 = guide impedance loaded with the lens dielectric. We assume that there is a material ε_2, and a length l_2 that "matches" the exterior impedance with the interior impedance. Using a transmission line analog, as shown in Figure 4, a match is simply a condition where no reflections occur, in the time

harmonic sense, at the interface. The reflection coefficient between the exterior and the second medium is

$$\Gamma = \frac{Z_0 - Z_2}{Z_0 + Z_2} \tag{2.15}$$

and the reflection coefficient, transformed back to the beginning of section two is

$$\Gamma(z = -l_2) = \frac{Z_0 - Z_2}{Z_0 + Z_2} e^{-j2\beta_2 l_2} \tag{2.16}$$

The impedance "looking into" the second section from the first is

$$Z^{in}(z = -l_2) = Z_2 \frac{1 + \Gamma(z = -l_2)}{1 - \Gamma(z = -l_2)} \tag{2.17}$$

which after some rearranging becomes

$$Z^{in}(z = -l_2) = Z_2 \frac{(Z_0 + Z_2) + (Z_0 - Z_2)e^{-j2\beta_2 l_2}}{(Z_0 + Z_2) - (Z_0 - Z_2)e^{-j2\beta_2 l_2}} \tag{2.18}$$

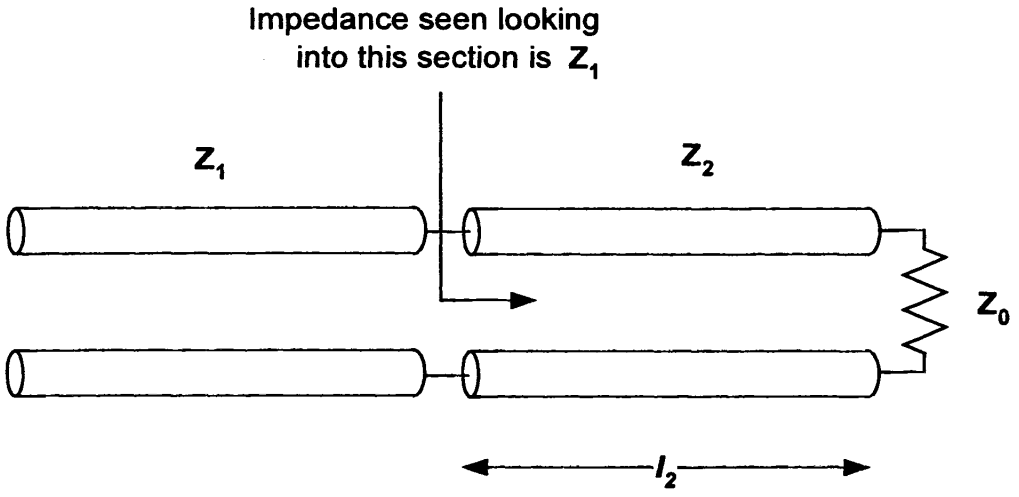

Figure 4. Transmission line analog of the impedance matching section.

It is the objective that $Z^{in}(z = -l_2) = Z_1$ so that no reflections occur at the interface between the first and second regions. Without showing rigorously that it is true [Ref. 8] it can be shown that this happens when the length of the second region is a quarter of a wavelength in the guide and region: $l_2 = \lambda_{g2}/4$. Then, $e^{-j2\beta_2 l_2} = -1$ and

$$Z_1 = Z_2 \frac{(Z_0 + Z_2) - (Z_0 - Z_2)}{(Z_0 + Z_2) + (Z_0 - Z_2)} = Z_2 \frac{2Z_2}{2Z_0} \tag{2.19}$$

The condition for impedance match is then

$$Z_2 = \sqrt{Z_1 Z_0}\,, \tag{2.20}$$

which means that the dielectric constant for the second region is $\varepsilon_2 = \sqrt{\varepsilon_1 \varepsilon_0}$. A schematic of a conical horn antenna with a collimating lens, a COBRA lens and an impedance matching lens is shown in Figure 5.

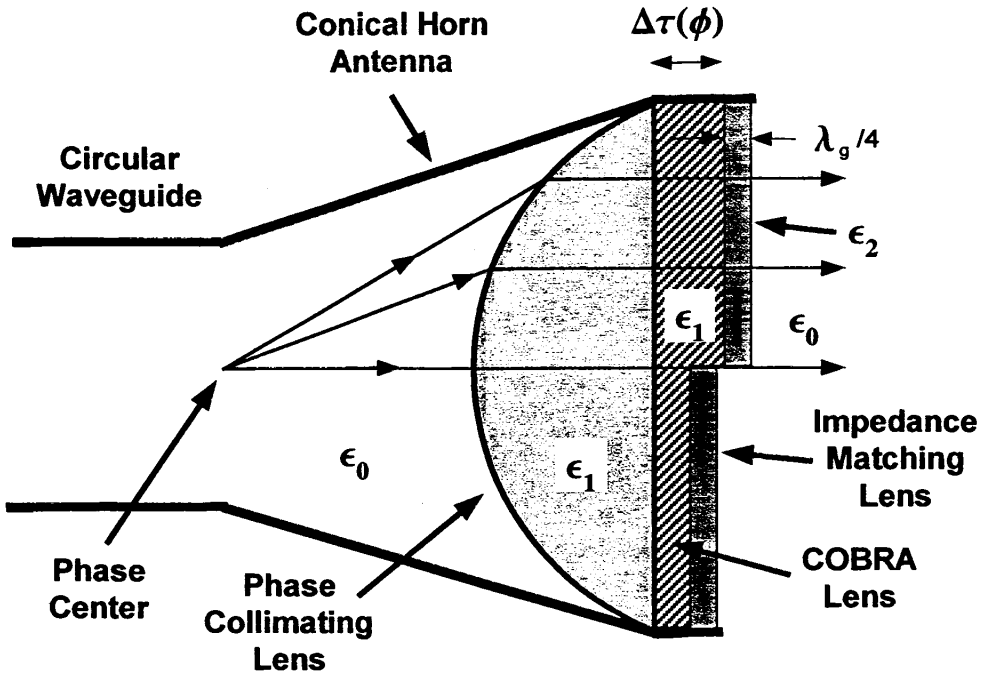

Figure 5. Architecture of a COBRA lens for a conical horn antenna.

We have noted that impedance matching at the front surface is less of a problem. But in some cases the transmission line impedance mismatch at the front surface of the lens is mitigated by the Brewster angle effect. For the case where the magnetic field is parallel to the dielectric boundary there is total transmission when the angle of incidence is

$$\theta_1 = \arctan\left(\sqrt{\varepsilon_{r2} / \varepsilon_{r1}}\right) \tag{2.19}$$

as indicated in Figure 6. The angle of transmission is given by

$$\sin(\theta_2) = \sin(\theta_1)/\sqrt{\varepsilon_{r2}/\varepsilon_{r1}}\,. \tag{2.20}$$

For a typical value of lens relative dielectric constant $\varepsilon_{r2} = 2.5$, $\theta_1 = \arctan\left(\sqrt{2.5}\right)$ $= 57.69^0$, and $\sin(\theta_2) = \sin(59.69)/\sqrt{2.5} = 0.546$. Then $\theta_2 = \arcsin(0.546) = 33.09^0$. For horn geometries of practical interest the Brewster angle will most likely occur close to the wall of the horn – where the electric field is at or near its maximum. For this case the field rays incident on the portion of the lens close to its inner wall will undergo total transmission.

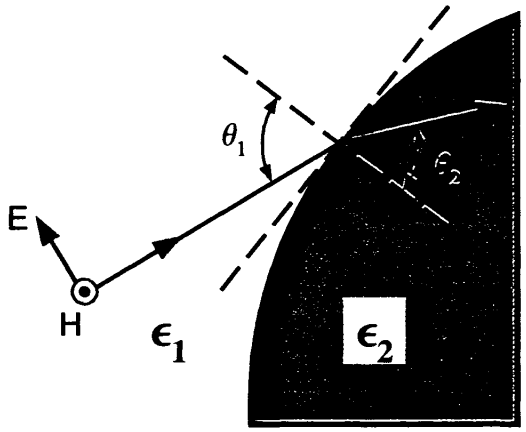

Figure 6. The geometry of the interior interface of the lens.

2.5 *Design Example*

We will conclude this section with a design example, using realistic parameters, that illustrates the use of a N = 4 COBRA lens designed to operate at 1.3 GHz. Let the diameter of a circular waveguide $= 2r = 9in$. A conical horn antenna with length = $l = 3r = 13.5in$ and aperture diameter = $2a = 4r = 18in$ terminates the waveguide. As discussed earlier the phase center of the antenna is assumed (approximated) to be located on the axis of the guide / antenna at the interface between the two. A lens with $\varepsilon_r = 4.54$ (fiberglass at 300 MHz) fits in the end of the conical horn. The parameters of the lens are as follows. The needed focal length can be found

$$f = \frac{2r(\sqrt{\varepsilon_r}\cos\theta - 1)}{\sqrt{\varepsilon_r} - 1)} = \frac{2(4.5)(\sqrt{4.54}\cos(18.43) - 1)}{\sqrt{4.54} - 1} = 8.130 \text{ in} \tag{2.21}$$

The lens radius is given as $a = 9$ inches, and the F-number for the lens is then $F = f/2a = 0.451$. The profile of the COBRA lens is given as

$$\Delta\tau(\varphi) = \lambda_g \frac{(n-1)}{N} \qquad \text{for } n = 1,2,\ldots,N. \tag{2.22}$$

where $\lambda_0 = 23$ cm = 9.055 in, and

$$\lambda_g = \frac{\lambda_0}{\sqrt{1-\left(\frac{2.405}{a}\right)^2\left(\frac{\lambda_0}{2\pi}\right)^2}} = \frac{9.055}{\sqrt{1-\left(\frac{2.405}{9}\right)^2\left(\frac{9.055}{2\pi}\right)^2}} = 9.812 \text{ in.} \tag{2.23}$$

Note that we have used the aperture radius and assumed TM_{01} mode-like propagation to the aperture. The COBRA step thickness is then:

$$\tau(\phi) - inches = \begin{cases} 0, & 0 \le \phi < \pi/2 \\ 2.45, & \pi/2 \le \phi < \pi \\ 4.91, & \pi \le \phi < 3\pi/2 \\ 7.36, & 3\pi/2 \le \phi < 2\pi \end{cases} \tag{2.24}$$

The impedance matching section should have a dielectric constant of $\varepsilon_r = 2.13$ (use Teflon, $\varepsilon_r = 2.1$) and will have a thickness of $l_2 = \lambda_g / 4 = 2.45$ inches. A rough estimate of the power lost due to impedance mismatch at the interior surface is $|\Gamma| = \frac{\sqrt{4.54}-1}{\sqrt{4.54}+1} = 0.361$, which gives a power loss ratio due to impedance mismatch of $|\Gamma|^2 = (0.361)^2 = 0.130$. A fully illuminated aperture of this size would have a gain of

$$G = 4\pi\frac{A}{\lambda^2} = 4\pi\frac{\pi(9)^2}{(9.06)^2} = 38.96 = 15.91 \text{ dB} \tag{2.25}$$

The COBRA lens divides the boresight power into two linear, orthogonal polarizations, with the proper phase relationship to yield circular polarization. The gain of each linear polarization is –3.92 dB less [Ref. 1] than the fully illuminated (or peak) linear gain. Then, the gain of each polarization alone will be

$$G_L = = 15.91 \text{ dB} - 3.92 \text{ dB} = 12 \text{ dB} \tag{2.26}$$

3. NUMERICAL SIMULATION OF A COBRA LENS DESIGN

In this section we simulate, via the Finite-Difference Time-Domain (FDTD) method, the electromagnetic behavior of a conical horn antenna with various COBRA lenses. The basic geometry of interest (a conical horn antenna without a lens) is shown in

Figure 7. There, a circular waveguide with a diameter of 13.48 inches = 34.24 cm is depicted. The waveguide transitions to a 24 inch = 60.98 cm diameter circular aperture along a 14.45 inch = 36.70 cm axial length.

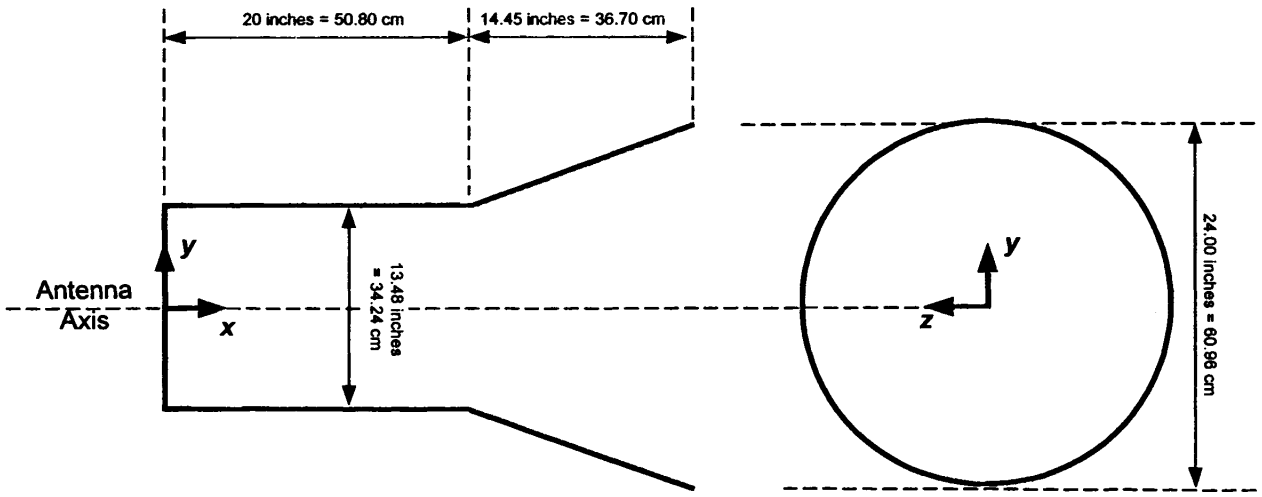

Figure 7. The geometry of the conical horn antenna of interest.

An FDTD model of the geometry was defined with the simulation domain specified to be 45 in × 35 in × 35 in. The dimensions of the rectangular cells of the grid ($\Delta x, \Delta y$ and Δz) were specified as $\Delta x = 0.25$ in, $\Delta y = 0.25$ in and $\Delta z = 0.25$ in. The center frequency of interest is $f_0 = 1.3$ GHz, with a wavelength of $\lambda_0 = 9.08$ in = 23.1 cm. Standard finite difference modeling practices suggest a cell size $\frac{\lambda}{20} < \Delta < \frac{\lambda}{10}$, or for the present case (in free space) $\frac{9.08}{20} = 0.454 < \Delta < 0.908 = \frac{9.08}{10}$ in. The cell size for our grid is much smaller, $\Delta x = \Delta y = \Delta z = 0.25$ in , or $\Delta x = \Delta y = \Delta z \approx \lambda/36$, and should be sufficient even when we introduce dielectric materials into the domain.

The computed far field gain for E_θ component in the plane at 1.3 GHz ($\theta = 90°, -90 \le \phi \le +90$) for the N = 1 conical horn (no lens) is shown in Figure 8, the peak gain is indicated as 11.56 dB.

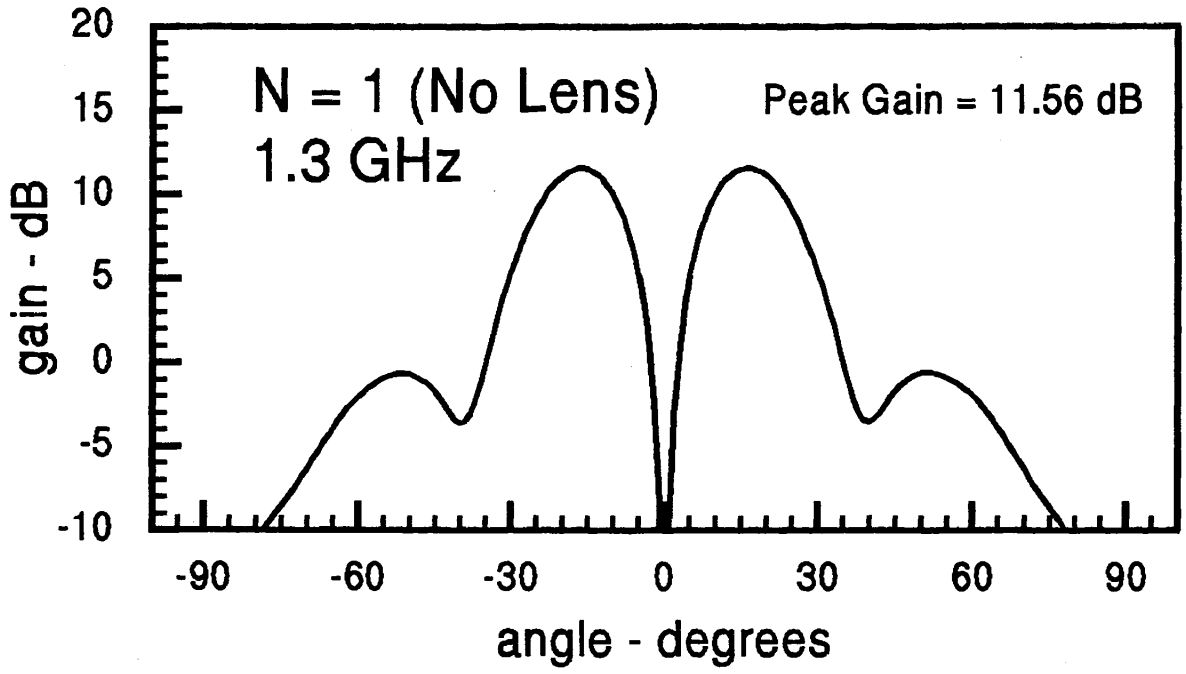

Figure 8. The computed far field pattern of the conical horn: E_θ component in the plane: $\theta = 90^\circ, -90 \le \phi \le +90$.

Next, an $N = 2$ lens was defined for the conical horn with an operating frequency = 1.3 GHz. The lens step size will be

$$l_1 = 0, \quad l_2 = \frac{\pi}{\beta}\frac{1}{\sqrt{\varepsilon_r - 1}} = \frac{\pi}{2\pi}\frac{\lambda}{\sqrt{\varepsilon_r - 1}} = \frac{\lambda}{2}\frac{1}{\sqrt{\varepsilon_r - 1}} \tag{3.1}$$

where λ_g = mode wavelength in the guide, and $\varepsilon_r = 2.5$ is the relative dielectric constant of the lens. Then

$$l_1 = 0, \quad l_2 = \frac{\lambda}{2}\frac{1}{\sqrt{\varepsilon_r - 1}} = \frac{9.49}{2}\frac{1}{\sqrt{2.5 - 1}} = 8.16 \text{ inches} \tag{3.2}$$

Half of the disk (half defined as a plane cut through the lens along the antenna axis), indicated in the figure as Region I, has a lens thickness of 3.00 inches. The other half, indicated as Region II, has a thickness of 11.16 inches. The lens geometry is shown in Figure 7. The lens has a thickness of one half wavelength in Region I to simulate a vacuum interface. Since the impedance is unaffected by a half wavelength section this portion of the lens has no effect on the aperture field. In Region II the lens has a thickness of the prescribed COBRA lens thickness plus the additional half wavelength. The extra material modifies the aperture field in the desired manner.

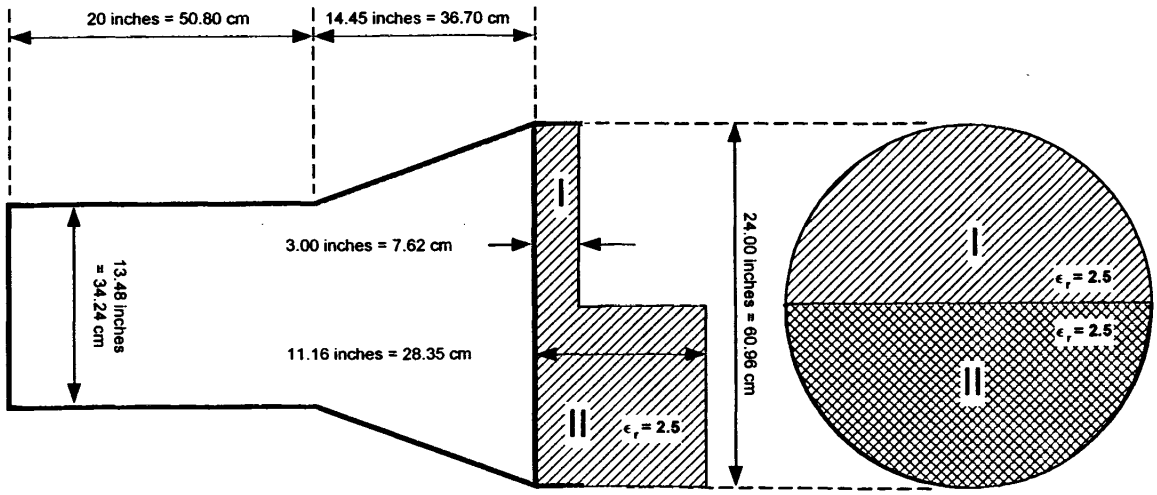

Figure 9. The geometry of the conical horn antenna with an N = 2 COBRA Lens.

The FDTD representation of the N = 2 COBRA Lens antenna was accomplished with the antenna axis is coincident with the global z-axis. Note that the feed for the model was at the base of the feed wire, between the wire and the back of the circular waveguide. A simulation at $f = 1300$ MHz was conducted, and the computed far field gain for both orthogonal electric field components in the elevation plane is shown in Figure 8. The peak gain is indicated as 13.51 dB, which is about 2 dB higher that the peak gain of the conical horn without a COBRA lens.

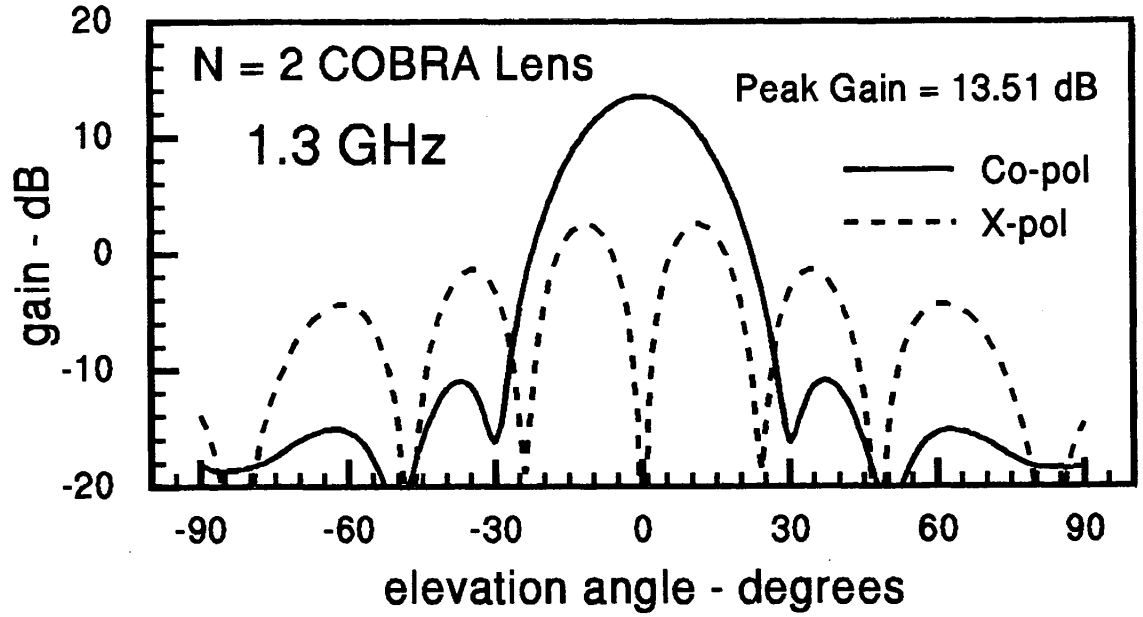

Figure 10. The computed far field pattern of both components of the electric field of the conical horn with a N = 2 COBRA Lens.

An optimization of the N = 2 design was attempted and consisted of the addition of a collimating lens added to the back of the N = 2 COBRA lens. Shown in Figure 11 is the magnitude of the electric field found from an FDTD simulation of the N = 2 COBRA lens. The simulation showed a wave front reaching the lens that is spherical-like in nature. A collimating lens was designed to straighten out the phase as the wavefront arrives at the aperture. The collimating lens will attach to the COBRA lens on the interior side (toward the circular waveguide) and will be composed of the same material as the COBRA lens. The specifics of the design are not recounted here. In Figure 12 is depicted the N = 2 COBRA Lens antenna with a collimating surface. The simulation was run again with the geometry shown in Figure 12. The electric field magnitude at a cross section of the geometry including the antenna axis is shown in Figure 13. One notes that the phase has been straightened out to some degree. Unfortunately, in this case the computed gain did not increase over the case where no collimating lens was used. The collimating lens may increase performance in apertures that are electrically larger. Also note that the finite difference model did not include a quarter wave transformer for impedance matching (as described in Section 2.4). The mismatch for lens materials with low relative dielectric constants is small, and the performance enhancement for lenses with impedance matching sections is small. For all cases presented in this note the relative dielectric constant was ~ 2.5, and no finite difference models of the antennas and lenses included impedance matching sections.

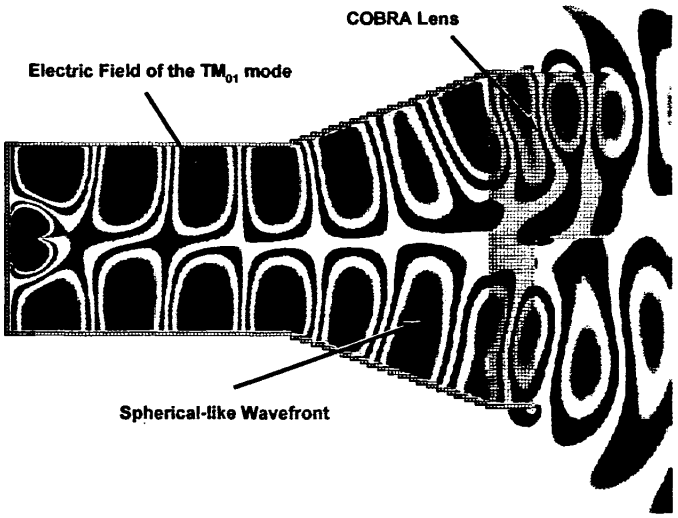

Figure 11. The simulation of the N = 2 COBRA lens showed a spherical-like wave front reaching the lens.

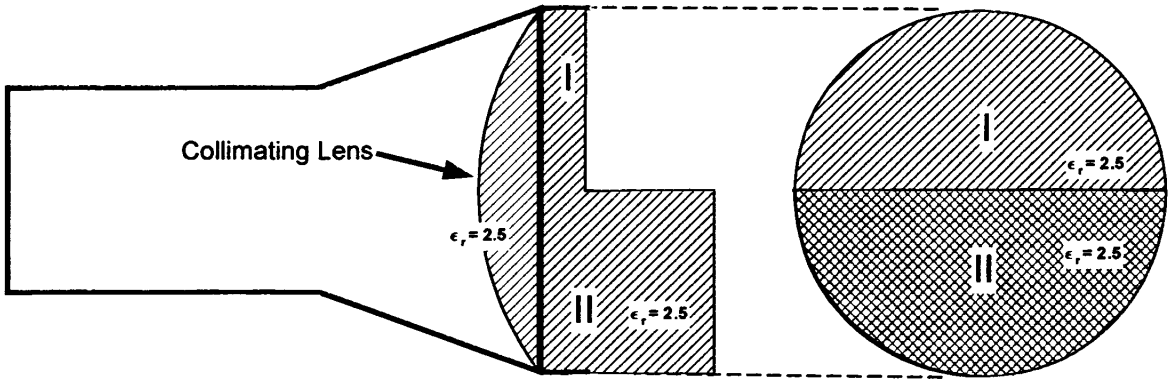

Figure 12. The N = 2 COBRA Lens with collimating lens added to the rear.

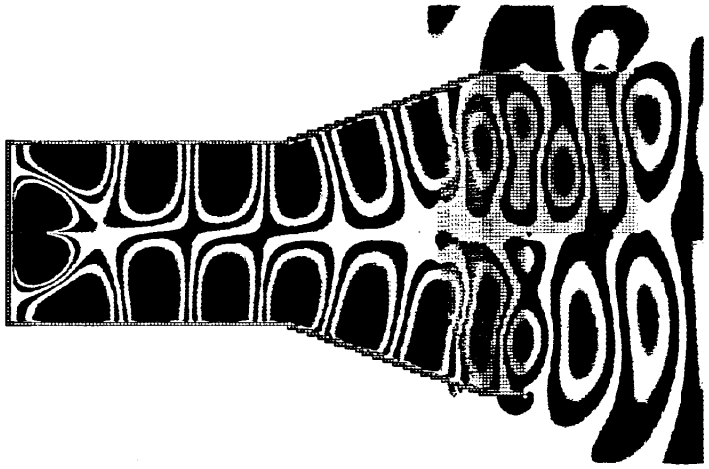

Figure 13. The electric field of a conical antenna with COBRA and collimating lenses.

The theory of the COBRA antenna operation indicates that the minimum number of sectors needed to produce a boresight peak with circular polarization is N = 3. In order to minimize the largest step discontinuity between the sectors, a design for an N = 3 COBRA lens was conducted. The operational parameters for the present case are: $N = 3$, operating frequency = 1.3 GHz, λ_g = mode vacuum wavelength in the guide = 9.19 inches (= 23.3 cm), and $\varepsilon_r = 2.5$ is the relative dielectric constant of the lens. Then

$$l_1 = 0 + 3 = 3 \qquad \text{inches,} \tag{3.3}$$

$$l_2 = \frac{(2-1)}{3}\frac{\lambda}{\left(\sqrt{\varepsilon_r}-1\right)} + 3 = \frac{1}{3}\frac{9.49}{\left(\sqrt{\varepsilon_r}-1\right)} + 3 = 8.44 \text{ inches, and} \tag{3.4}$$

$$l_3 = \frac{2}{3}\frac{9.49}{\left(\sqrt{\varepsilon_r}-1\right)} + 3 = 13.88 \text{ inches.} \tag{3.5}$$

Note that again, an additional length of 3 inches has been added to each section of the lens to simulate a vacuum interface. A schematic of the design is shown in Figure 14.

The finite difference representation of the N = 4 COBRA Lens antenna was accomplished, and the simulation conducted. The gain of the E_θ and E_ϕ components was computed for $-90 \le \theta \le +90, \phi = 0°, 90°$. These values are shown in Figure 15 and Figure 16, note the orientation of the sectors as indicated in the figures. These results show a pattern with a slightly squinted beam, but with a gain for each component of approximately 10 dB on boresight. The phase difference between the two components on boresight was approximately 90-degrees. The N = 3 COBRA, then, produces circular polarization on boresight, but not quite a boresight peak.

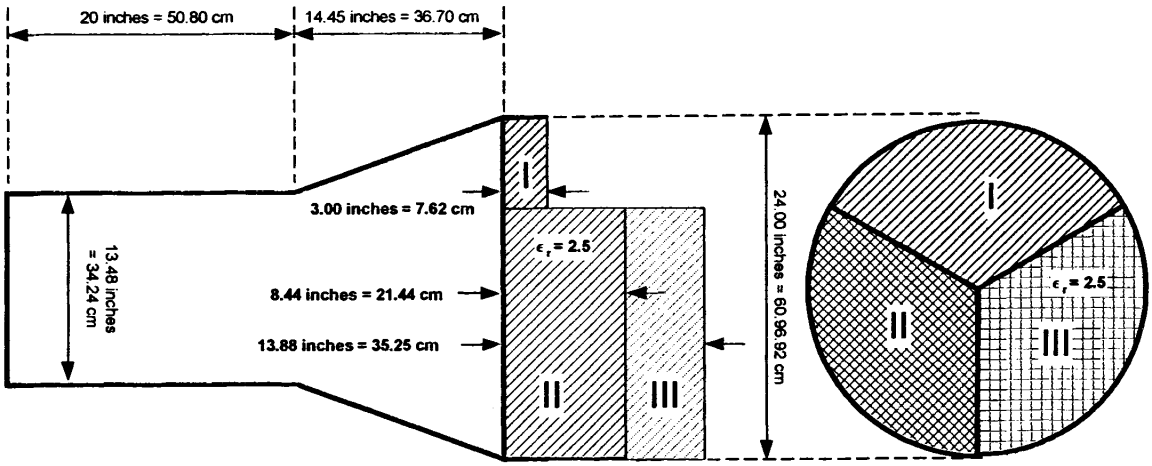

Figure 14. A schematic of the design of the N = 3 COBRA Lens antenna.

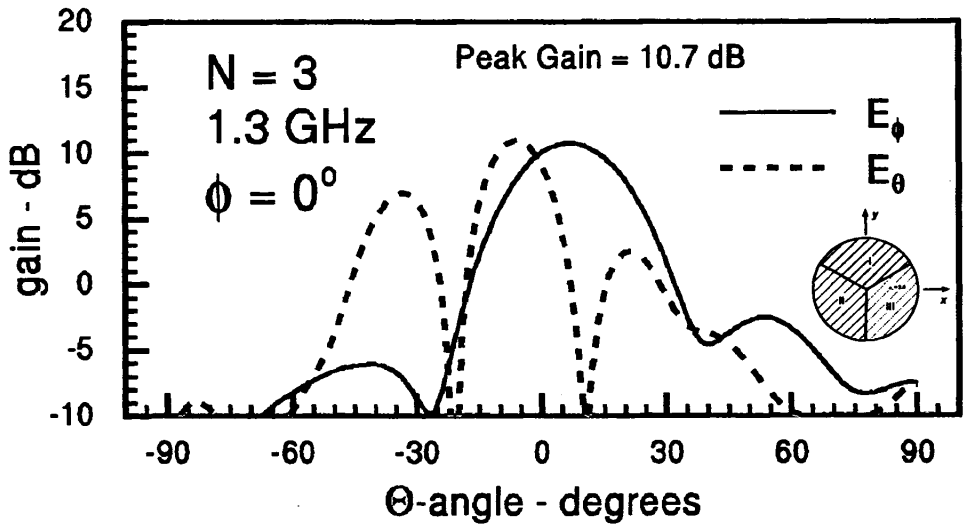

Figure 15. The computed gain of the of the E_θ and E_ϕ components of the N = 3 COBRA Lens for $\phi = 0°$ ($y = 0$). Orientation of the sectors is indicated.

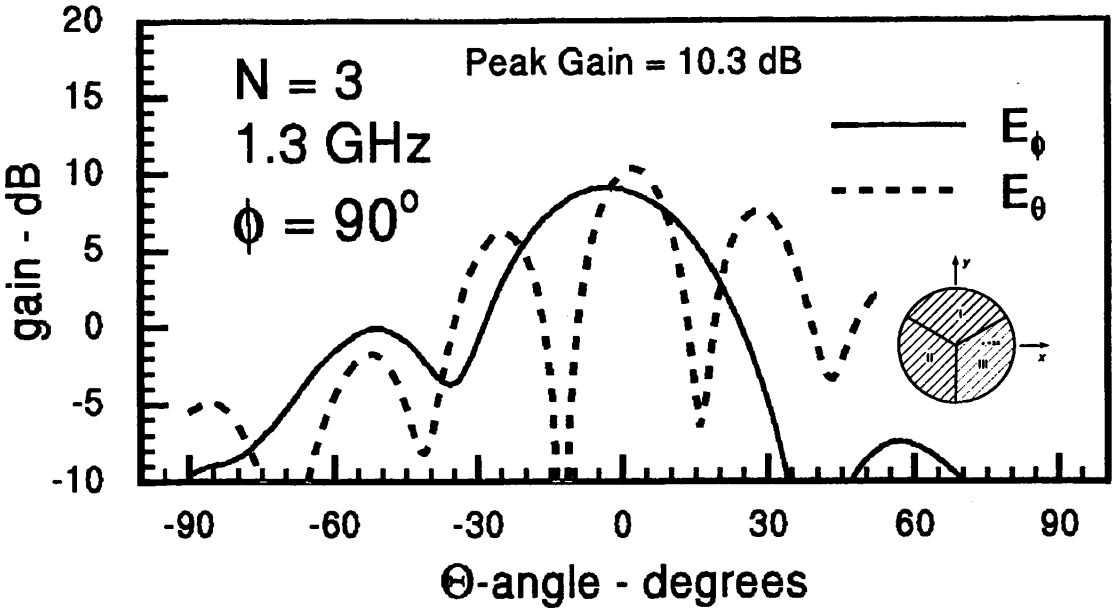

Figure 16. The computed gain of the of the E_θ and E_ϕ components of the N = 3 COBRA Lens for $\phi = 90^\circ$ ($x = 0$). Orientation of the sectors is indicated.

A design of the N = 4 COBRA Lens Antenna is shown in Figure 17. The sectors have been rotated 90-degress so that each far field component "sees" the same degree of physical discontinuity in the lens surface. Otherwise the lens thickness is the same for each sector.

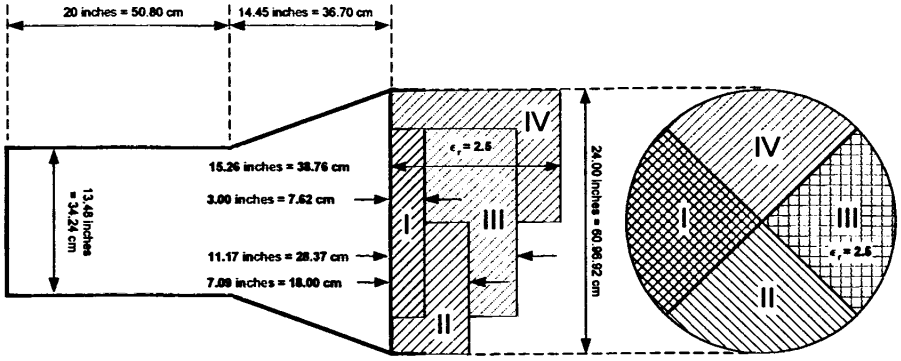

Figure 17. An alternate design of the N = 4 COBRA Lens Antenna. Sectors have been rotated 90-degrees.

The simulation was again run, and the gain of the E_θ and E_ϕ components was computed for $-90 \le \theta \le +90, \phi = 0^\circ$. These values are shown in Figure 18, note the orientation of the sectors as indicated in the figure. The gain figures for the E_ϕ and E_θ components are equal on boresight, and the phase difference is 113-degrees. The gain and phase difference between the principal components was computed as a function of

frequency. The gain difference, in dB, between the E_ϕ and E_θ components as a function of frequency on boresight is shown in Figure 19. The phase difference, in degrees, between the E_ϕ and E_θ components as a function of frequency on boresight is shown in Figure 20.

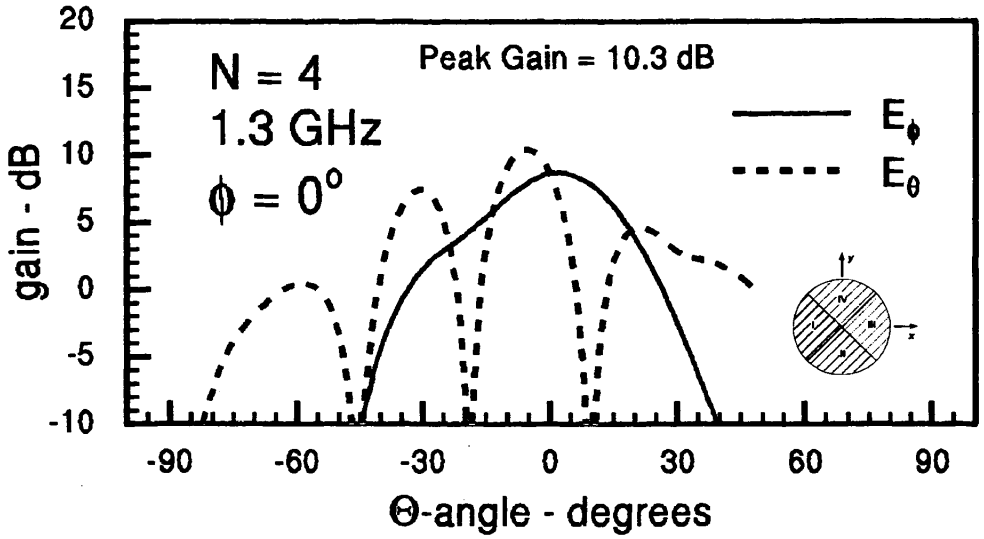

Figure 18. The computed gain of the of the E_θ and E_ϕ components of the N = 4 COBRA Lens for $\phi = 0°$. Orientation of the sectors is indicated.

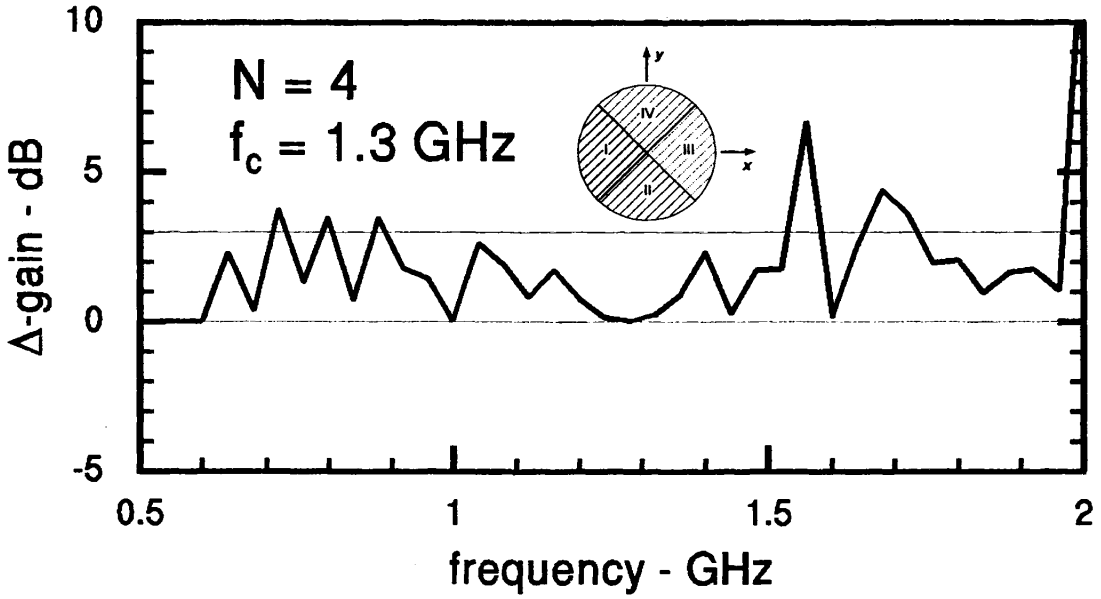

Figure 19. The difference in computed gain of the E_θ and E_ϕ components of the N = 4 (rotated) COBRA Lens. Orientation of the sectors is indicated.

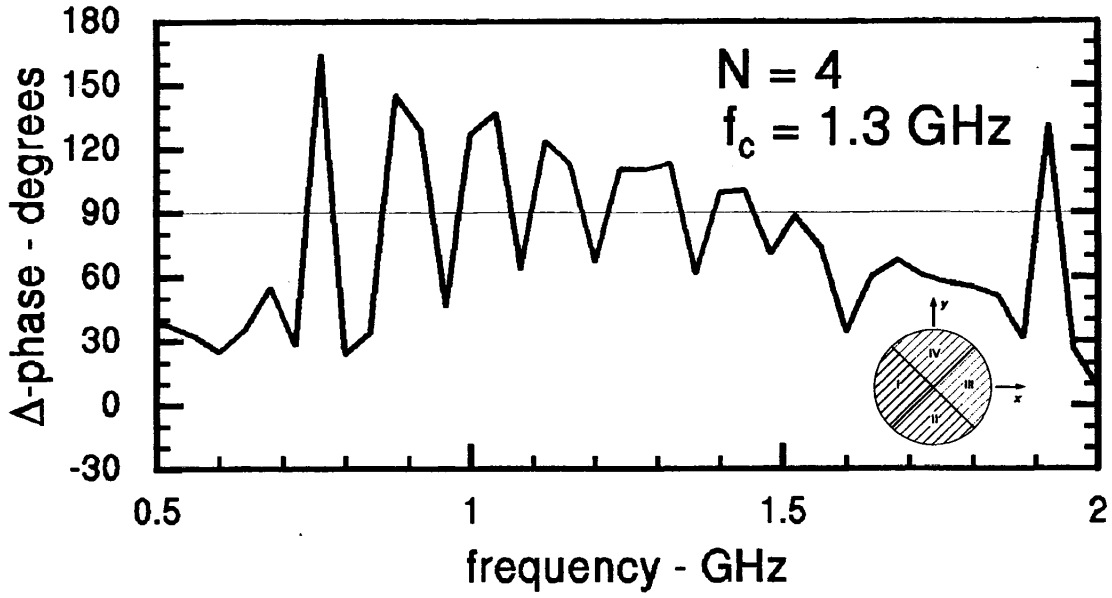

Figure 20. The difference in the computed phase of the E_θ and E_ϕ components of the N = 3 COBRA Lens. Orientation of the sectors is indicated.

II. Conclusions

It was found that the COBRA Lens design can modify the aperture electric field distribution in a manner that produces a boresight peak, with linear or circular polarization. The comparisons of the gain and efficiencies associated with the different COBRA configurations, for $\lambda = 1.3$ GHz and an aperture diameter = 24 inches. are shown in Table 1. The gain figures are given in terms of total power per period, and are indicated as G_L for the gain associated with linear polarization and G_C for an equivalent gain associated with circular polarization.

Table 1. Comparisons of the gain and efficiencies associated with the different COBRA configurations for $\lambda = 1.3$ GHz, and aperture diameter = 24 inches.

	$4\pi A/\lambda^2$	N = 1	N = 2	N = 3: E_θ, E_ϕ	N = 4: E_θ, E_ϕ
Gain Lin - dB	18.4	Null	13.5	10 , 10	9.5 , 9.5
Gain Cir - dB	18.4	Null	13.5	13	12.5
Efficiency - Lin	100 %	0 %	32 %	14.4 %	12.9 %
Efficiency - Cir	100 %	0 %	32 %	28.8 %	25.8 %

REFERENCES

1. "Coaxial Beam-Rotating Antenna (COBRA) Concepts," C. Courtney and C. E. Baum, AFRL Sensor and Simulation Note 395, April 1996.
2. "Coaxial Beam-Rotating Antenna (COBRA) Prototype Measurements," C. Courtney, et al., AFRL Sensor and Simulation Note 408, July 1997.
3. "Design and Measurement of a Cassegrain-type Coaxial Beam-Rotating Antenna," C. Courtney, et al., AFRL Sensor and Simulation Note 427, November 1998.
4. "Design and Optimization of a Conical Transmission-Line Feed for a Coaxial Beam-Rotating Antenna," C. Courtney, et al., AFRL Sensor and Simulation Note 429, September 1998.
5. "Design, Fabrication and Measurement of a Conical Transmission-Line Fed, Cassegrain Coaxial Beam-Rotating Antenna," C. Courtney, et al., AFRL Sensor and Simulation Note 429, March 2000.
6. "The coaxial beam-rotating antenna (COBRA): theory of operation and measured performance," C. Courtney and C. E. Baum, IEEE Trans. on Antenna and Propagation, vol. 48, no. 2, Feb., 2000.
7. *Antennas and Radiowave Propagation*, R. E. Collin, McGraw-Hill, New York, 1985.
8. *Microwave Engineering*, D. Pozar, Addison-Wesly, Reading, Mass., 1993.